Supplementary Material

Unveiling Anion-Induced Folding in Tripodal Imidazolium Receptors by Ion-mobility Mass Spectrometry

Cristian Vicent,[*a] Adriana Valls,[b] Jorge Escorihuela,[c] Belén Altava[*b] and Santiago Luis[b]

[a.] *Servei Central d'Instrumentació Científica (SCIC), Universitat Jaume I, Avda. Sos Baynat s/n, 12006 Castellón, Spain. E-mail address: barrera@uji.es*

[b.] *Departamento de Química Inorgánica y Orgánica, Universitat Jaume I, Av. de Vicent Sos Baynat, s/n 12071, Castellón, Spain.*

[c.] *Departamento de Química Orgánica, Universitat de València, Avda. Vicent Andrés Estellés s/n, 46100 Burjassot, València, Spain.*

Table of contents:

1.- General Information

Reagents and solvents, including NMR solvents, were purchased from commercial suppliers and were used without further purification. NMR spectra were recorded on a Varian Innova 500 MHz or on a Bruker 400 NMR spectra at room temperature with CD_3OD as NMR solvent. All values of the chemical shift are in ppm regarding the δ-scale and referenced to the non-deuterated residual solvent. Compound [**3**]Br_3 was synthetized as previously described.[1]

Synthesis of [**1**]Br_3**.** 2-(1H-imidazol-1-yl)-N-methyl-3-phenylpropanamide (0.301 g, 1.31 mmol, 4 equiv) and 1,3,5-tris(bromomethyl)benzene (0.117 g, 0.327 mmol, 1 equiv) were dissolved in acetronitrile (0.4 M, 3.3 mL) in a microwave tube. The conditions of this reaction in the Microwave instrument were: 150 ºC, 1h and 120W. The liquid obtained was evaporated and washed with ethyl acetate at the vaccum. The reaction gave a brown solid product (0.26 g, 77.7%). $[\alpha]_D^{25}$ = 14.23 (c = 0.011, MeOH). IR (ATR): ν˜max = 3396, 3353, 3232, 3066, 1677, 1554 cm^{-1}. ^1H NMR (400 MHz, Methanol-d4) δ = 9.51 (s, 3H), 7.76 (d, J = 1.8 Hz, 6H), 7.62 (s, 3H), 7.40-7.15 (m, 15H), 5.58 – 5.44 (m, 9H), 3.56 (dd, J = 13.9, 6.6 Hz, 3H), 3.42 (dd, J = 13.9, 9.4 Hz, 3H), 2.73 (s, 9H). ^{13}C NMR (101 MHz, MeOD) δ 167.58, 136.14, 134.77, 129.62, 128.85, 128.52, 127.24, 122.57, 122.13, 64.00, 51.97, 38.61, 25.30. ESI (+) MS: *m/z* 441.71 [**1** + Br]$^{2+}$. Calculated for $C_{48}H_{54}N_9O_3$: C 55.18, H 5.21, N 12.07; found $C_{48}H_{54}N_9O_3 \cdot H_2O$: C 54.1, H 5.62, N 11.57.

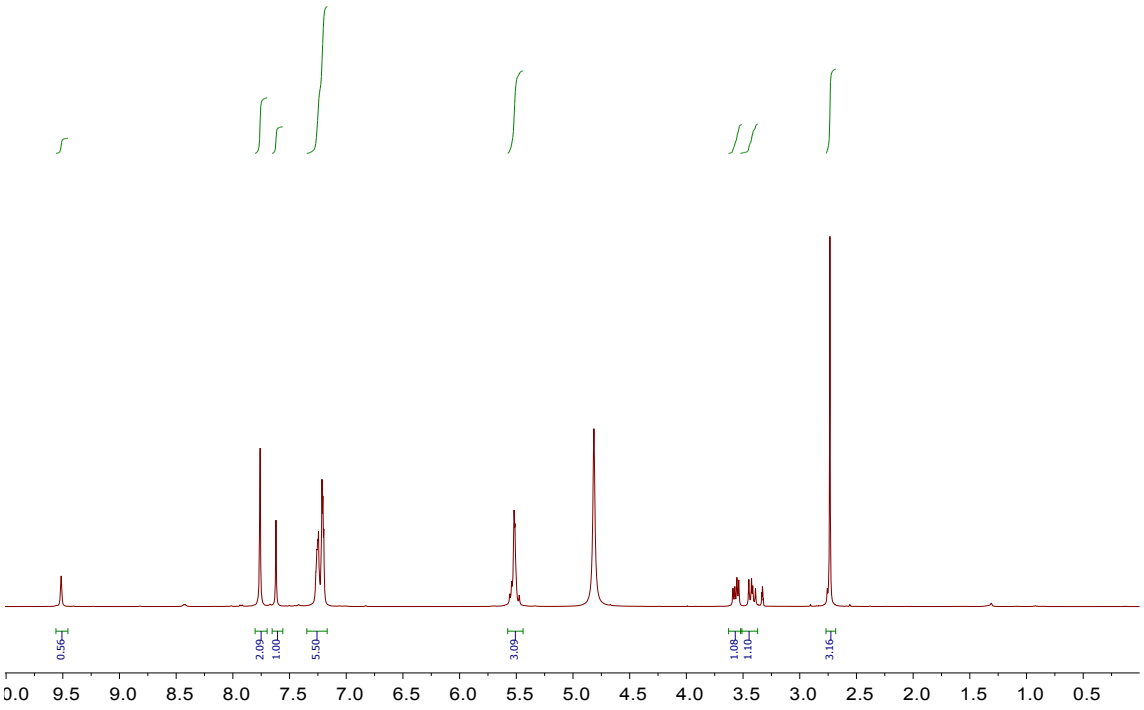

Figure S1. 1H NMR spectrum of [**1**]Br_3 in CD_3OD

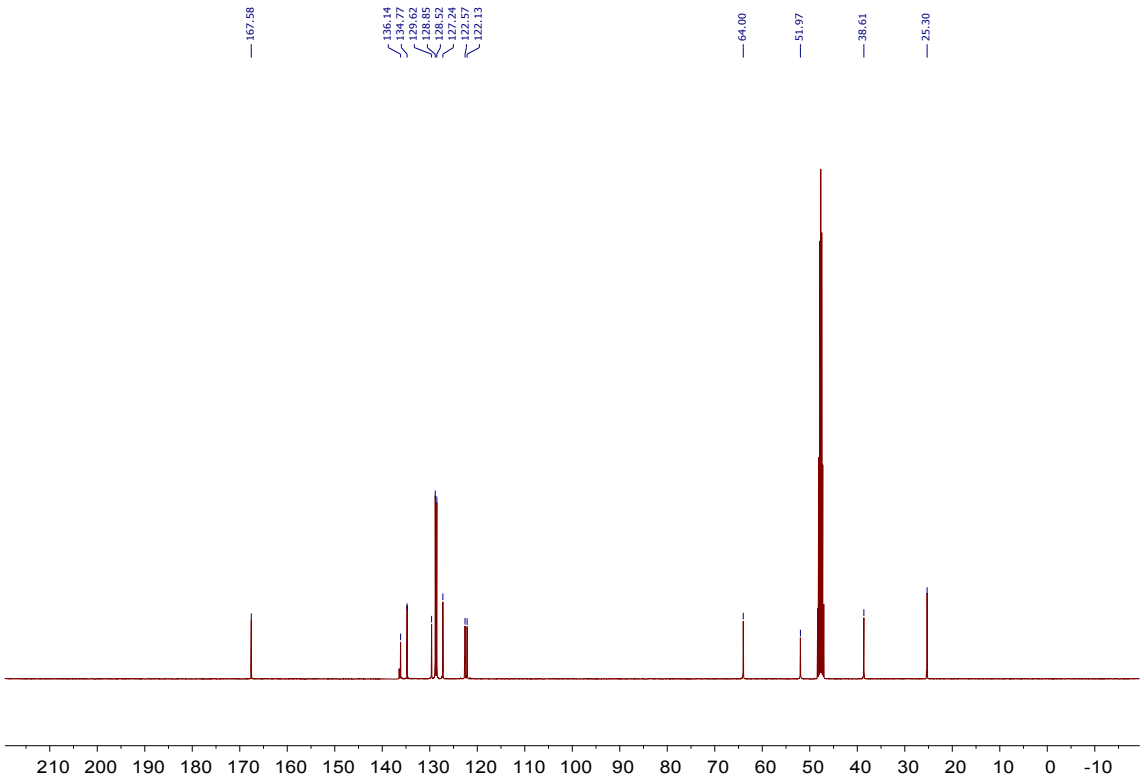

Figure S2. $^{13}C\{^1H\}$ NMR spectrum of [**1**]Br_3 in CD_3OD

Synthesis of [2]Br_3: (*S*)-N-butyl-2-(1H-imidazol-1-yl)-3-methylbutanamide (0.201 g, 0.914 mmol, 3.3 equiv) and 1,3,5-tris(bromomethyl)benzene (0.097 g, 0.273 mmol, 1 equiv) were dissolved in acetronitrile (0.4 M, 2.65 mL) in a microwave tube. The conditions of this reaction in the Microwave instrument were: 150 ºC, 1h and 120W. The liquid obtained was evaporated and washed with ether at the vaccum and, then, with ethyl acetate. The reaction gave a brown solid product (0.274 g, 97.7%): mp 99 ºC; $[\alpha]_D^{25}$ = 10.8 deg cm^3 g^{-1} dm^{-1} (c = 0.011 g cm^{-3}, MeOH). ^{1}H NMR (400 MHz, Methanol-d_4, δ): 9.30 (s, 3H), 8.67 (s, NH), 7.74 (t, *J* = 1.8 Hz, 3H), 7.65 (t, *J* = 1.8 Hz, 3H), 7.60 (s, 3H), 5.55 (s, 6H), 4.69 (d, *J* = 10.0 Hz, 3H), 3.40-3.24 (m, 6H), 2.44 (m, *J* = 9.7, 6.5 Hz, 3H), 1.51 (m, 6H), 1.33 (m, 6H), 0.97 (d, *J* = 6.7 Hz, 9H), 0.82 (t, *J* = 7.3 Hz, 9H), 0.77 (d, *J* = 6.7 Hz, 9H), ppm; ^{13}C NMR (101 MHz, Methanol-d_4, δ): 167.2, 167.1, 136.3, 129.7, 122.6, 122.5, 122.4, 68.9, 68.9, 52.1, 39.3, 39.1, 31.8, 31.8, 30.8, 30.8, 19.7, 17.9, 17.5, 12.6.ppm; IR (ATR): ν˜max = 3228, 3067, 2961, 2933, 2872, 1672, 1549, 1463, 1369, 1154 cm^{-1}. ESI (+) MS: *m/z* 432.75 [**2** + Br]$^{2+}$. Anal. calcd for $C_{42}H_{72}N_9O_3Br_3$: C 68.67, H 9.22, N 16.02 found C 67.42, H 9.43, N 16.24.

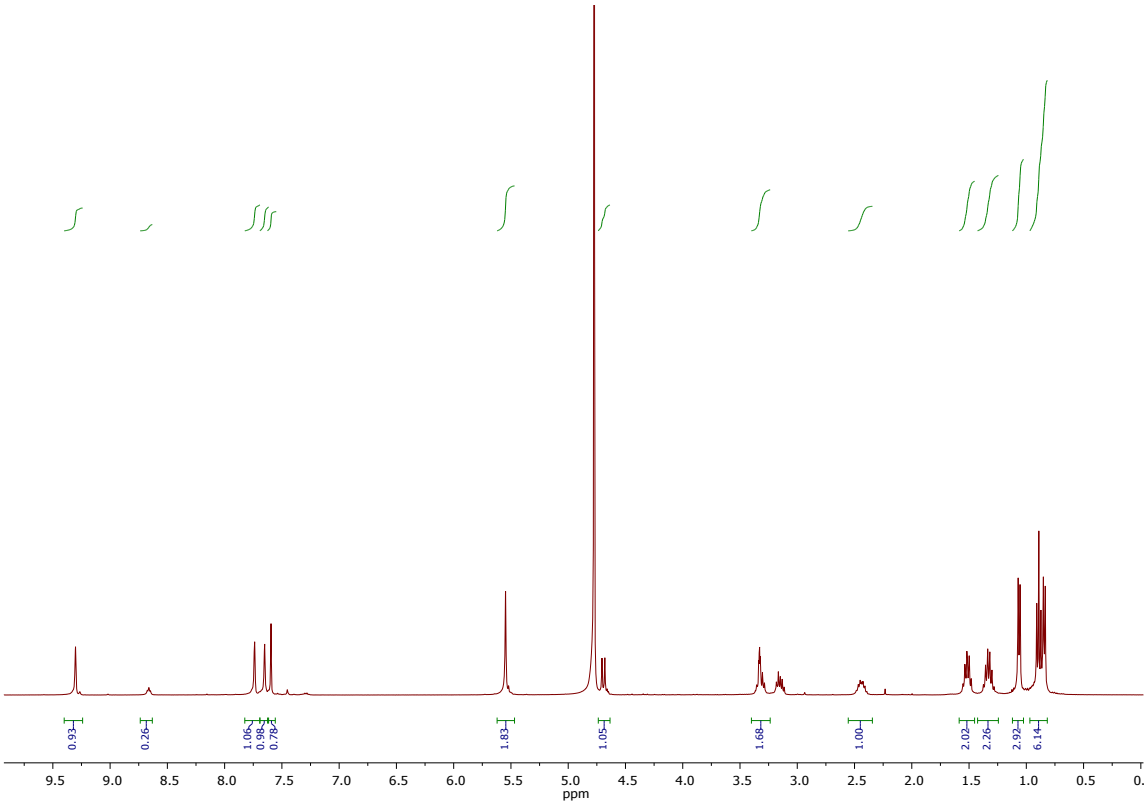

Figure S3. ^{1}H NMR spectrum of [**2**]Br_3 in CD_3OD

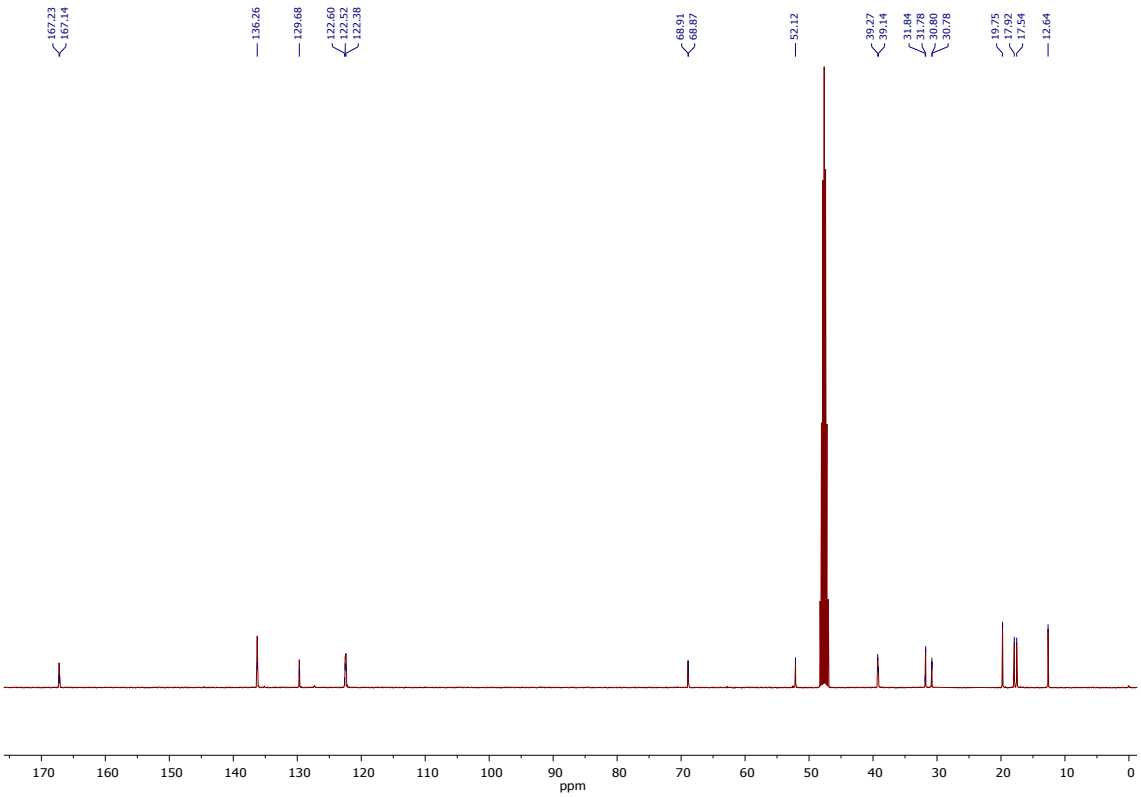

Figure S4. $^{13}C\{^{1}H\}$ NMR spectrum of [**2**]Br_3 in CD_3OD

2.- Electrospray Ionization Mass Spectrometry

Experiments were performed using a SYNAPT XS High Definition Mass Spectrometer (Waters Corporation, Manchester, UK) equipped with an electrospray ionization (ESI) source. After electrospray ionization, the ions generated are transmitted through the StepWave XS ion guide to the first quadrupole (Q), then to the traveling wave ion mobility (TWIM) cell, and finally analyzed with a time-of flight (TOF) mass analyzer. The ion mobility separation occurs through the so-called *triwave* device that operates with three regions: trap, ion mobility separation, and transfer with a helium cell located between the trap and ion mobility separation regions. A schematic view is given in scheme S1.

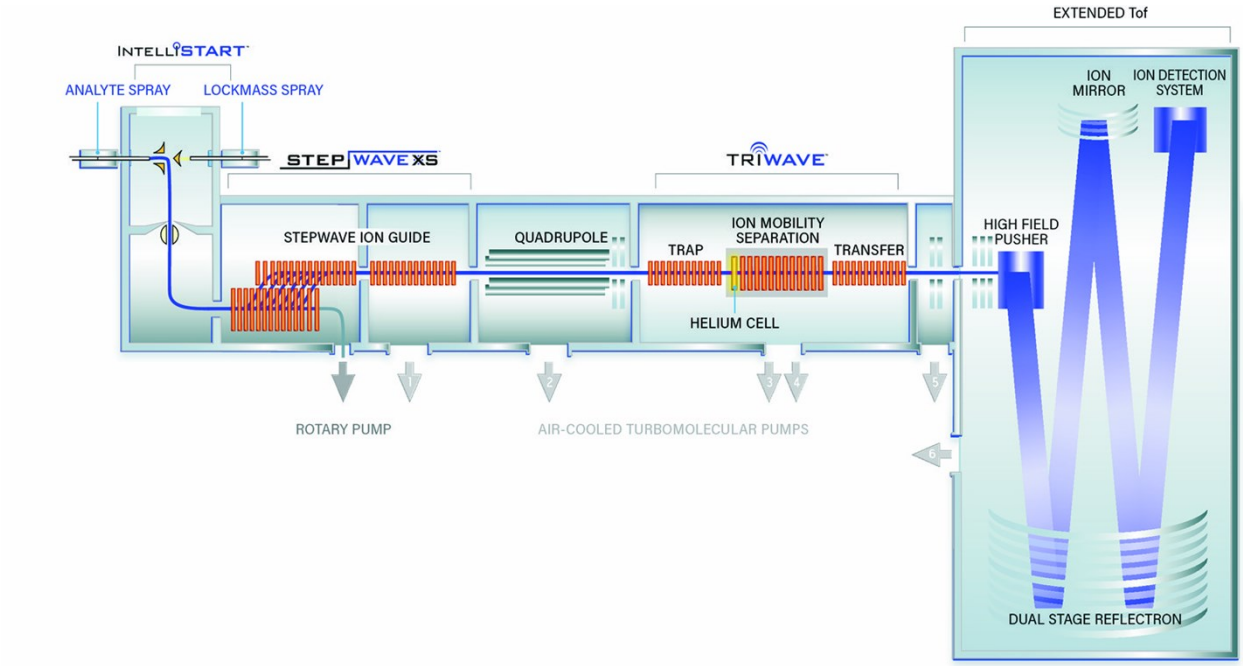

Scheme S1. Schematic view of the Synapt XS High Definition Mass Spectrometer. Reprinted from the waters.com webpage with permission from the Waters Corporation.

2.1.- Single-stage ESI-MS: a capillary voltage was set to 1.5 kV operated in the positive ionization mode and in the resolution mode. Source settings were adjusted to keep intact the supramolecular adducts of interest. Typical values were cone voltage 20 to 40 V and source offset 4 V;

source and desolvation temperatures were set to 110 and 350 ºC, respectively. Cone and desolvation gas flows were 150 and 500 (L/h), respectively. Sample solutions were prepared from stock chloroform 1mM solutions by 1000-fold dilution with chloroform:methanol (1:1) to reach the 1μM concentration and introduced directly to the ESI chamber through an external syringe pump at a flow rate of 5 $\mu L \cdot min^{-1}$. Calibration of the *m/z* axis up to m/z 1000 was performed using the routine implemented in intellistart from a mixture of sodium hydroxide and formic acid in 1:9 *v/v* H_2O:isopropanol. Comparison of experimental vs theoretical isotopic pattern was carried out using Masslynx 4.2 (SCN 982)

2.2 ESI TWIM-MS and CID prior to IM separation: the same sample solutions to that used for single-stage ESI-MS were investigated. Source settings were also identical to that described above for single-stage ESI-MS. The instrument was switched from TOF acquisition to mobility TOF acquisition mode and left for 30 minutes before recording TWIM mass spectra. The m/z 50-850 range was investigated and ion mobility separation settings were used as follows: the traveling wave height was set to 40 V and wave velocity was set to 650 m/s. The drift gas was nitrogen (N_2) at a flow rate set to 90 mL/min. The helium cell gas flow was 180.00 mL/min. IMS DC values were as follow: Entrance 20; Helium cell DC 50; Helium exit -20; Bias 3; Exit 0. Trap DC bias was 45 V; entrance, 3; Exit 0. CID experiments were performed by mass selecting the supramolecular $[M + X]^{2+}$ adducts of interest in the first quadrupole and increasing the collision voltage (V) in the trap region starting from 2 V and stepped by 2 V up to a maximum of 10 V. An isolation width of approximately 1 Da was selected (LM resolution set to 9). The only fragmentation channel was the release of HX neutral concomitant with the formation of $[M - H]^{2+}$. Ion mobility mass spectra of the $[M - H]^{2+}$ product ion were recorded after ion activation and displayed virtually the same ATD pattern and drift time to that observed for the $[M - H]^{2+}$ species recorded by ESI IM-MS.

The TWIM-MS data were processed using Masslynx 4.2 (SCN 982). All ions of interest displayed a gaussian-shaped arrival time distribution profile. Ion mobility spectra of the species of interest were extracted using a 0.15 Da mass window and were converted from waters.raw to .txt files. Gaussian fitting of the IM data was applied to improve the precision of the drift time measurements. The reported drift times values were obtained by Gaussian peak fitting using origin 6.0 (Microcal) rendering good correlation in all cases. Each sample was recorded by triplicate on the same day and the deviation in the drift time values was less than 0.5 %.

2.3 CCS Calibration

Several protocols have been reported for determining ^{TW}CCS based on traveling-wave drift times using calibrant ions whose ^{DT}CCS have been determined from drift tube IM experiments using both He or N_2. The CCS calibration protocol reported by Ruotolo was followed to convert drift times into CCS.[2] Polyalanine was chosen as calibrant to cover the transit time range of the doubly-charged ions of interest in the present work. Calibration of the IM-MS device for determining collision cross-sectional areas from drift time measurements was performed considering a series of multiply charged $(Ala_n + 2H)^{2+}$ species and their $^{DT}CCS_{N2}$ values were taken from the literature.[3] As the TWIMS device is operated with N_2 buffer gas, the obtained ^{TW}CCS values will be noted $^{TW}CCS_{N2}$. Drift times (t_D) were subjected to correction for mass-dependent and mass-independent flight times according to $t_D' = t_D - C * \frac{\sqrt{m/z}}{1000} - 0{,}9$ (C = 1.5 and the term 0.9 ms is the mass-independent time to account for the time of transit of one wave in the IMS and the transfer region). The literature CCS values were converted to CCS′ according to $CCS' = \frac{CCS\sqrt{\mu}}{z}$ where μ and z stands for the reduced mass of the collision partners and the charge state, respectively. The calibration curve is represented as CCS′ as a function of t_D' using a power law,[4] $CCS' = A \times (t_D')^B$. Constants A and B were subsequently

derived from the calibration plot and used to calculate cross-sectional areas ($^{TW}CCS_{N2}$) of unknown species from corrected drift time measurements extracted for specific *m/z* values from the data.

3 ESI IM mass spectra

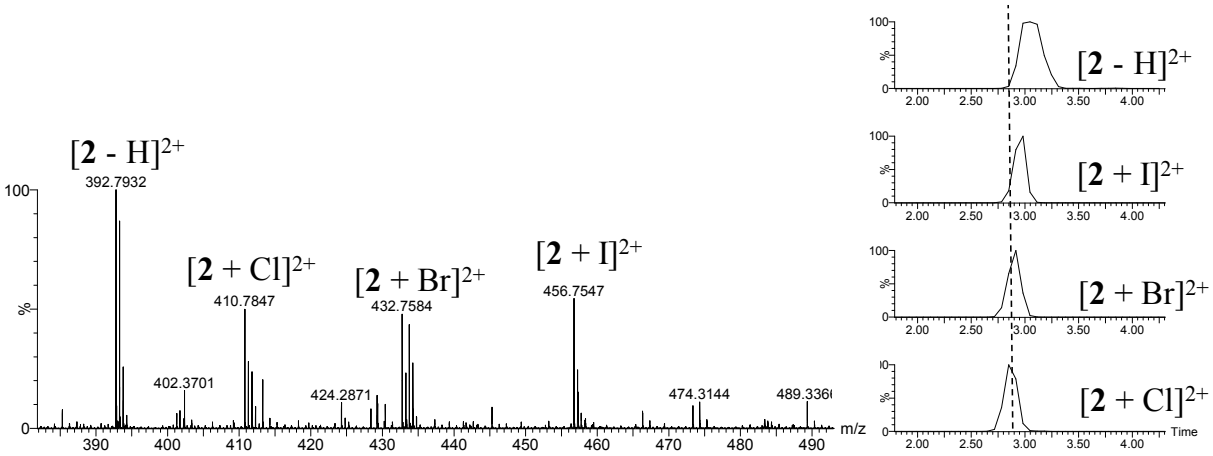

Figure S5. a) ESI IM mass spectrum of methanol 1μM solution of compound [**2**]Br_3 in the presence of three-equivalents of TEAX (X = Cl and I) recorded in the 50 to 850 range. The insets show the arrival time distribution for the most abundant isotopomer using an absolute window of 0.15 Da

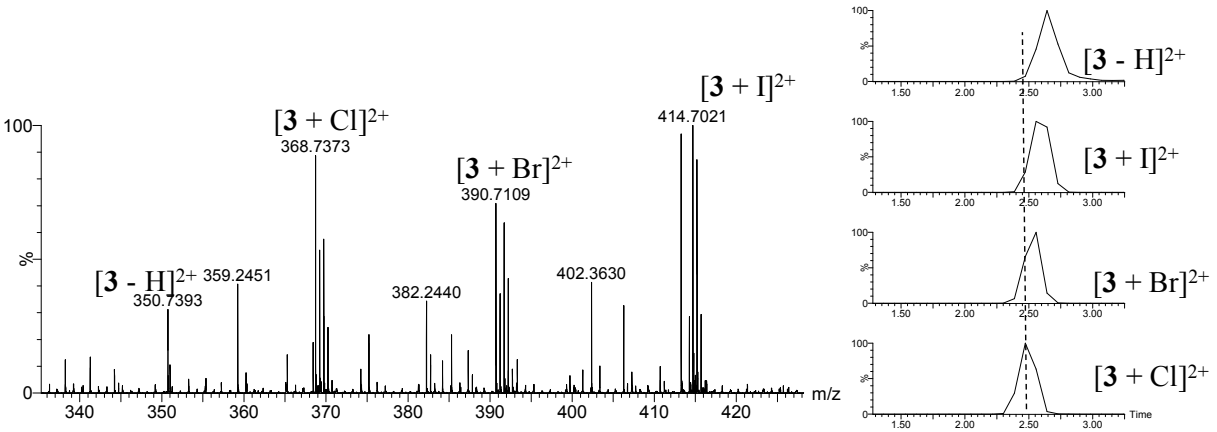

Figure S6. a) ESI IM mass spectrum of methanol 1μM solution of compound [**3**]Br_3 in the presence of three-equivalents of TEAX (X = Cl and I) recorded in the 50 to 850 range. The insets show the arrival time distribution for the most abundant isotopomer using an absolute window of 0.15 Da

4 Trajectory method (TM) CCS predictions.

IMoS 1.10 was used to calculate the average drag caused by the impinging N_2 gas molecules over the flight path of the dications of interest using the energy-minimized DFT structures as inputs.[5a] The potentials employed are standard TMLJ methods using a 4-6-12 potential. An Ion induced quadrupole potential (QPol option in IMos 1.10) was added to the 4-6-12 potential to account for ion-quadrupole interaction of the *atom-N_2* (atom = C, H, N, O) interaction.[5b] The N2 QPol Lennard-Jones parameters specified in IMos 1.10 for CHNO were considered accordingly. The number of rotations was 3 with 300000 gas molecules per rotations.

Table S1. Experimental $^{TW}CCS_{N2}$ values and simulated CCS using TM methods as implemented in the IMos software of the ionic species under study

	$^{TW}CCS_{N2}$ (Å^2)	Predicted CCS using TM methods
[**1** - H]$^{2+}$	323	321
[**1** + Cl]$^{2+}$	301	304
[**1** + Br]$^{2+}$	307	302
[**1** + I]$^{2+}$	312	309

5 NMR titration experiments

^{1}H NMR anion-binding studies were conducted for compound [**1**]Br_3 in $CDCl_3$ and tetrabutylammonium salts, namely (n-Bu4N)X (X = Cl, Br and I). Typically to 6mM stock solutions of the receptor were added increasing amounts of the anion salts. Characteristics plots of Δδ for compound **[1]**Br_3 against anion concentration are given in Figure S7. Stacked ^{1}H NMR spectra of titrations are also shown in Figures S8-10. Our [**1**]Br_3 system is singular and rather complex in spite of its apparent simplicity, because it already features three bromide anions binding to the tripodal receptor. For this reason, the distinctive chemical shift variation of the target resonances upon adding (n-Bu4N)X (X = Cl, Br and I) is a consequence of the competitive binding of bromide (present in the starting compound) and the titrating anion. The number of possible complex species is too large (as is the number of involved association constants). For this reason, all attempts to obtain binding constants with acceptable adjustments using the software package HypNMR2008 or the one suggested by reviewer 1, BindFit were unsuccessful

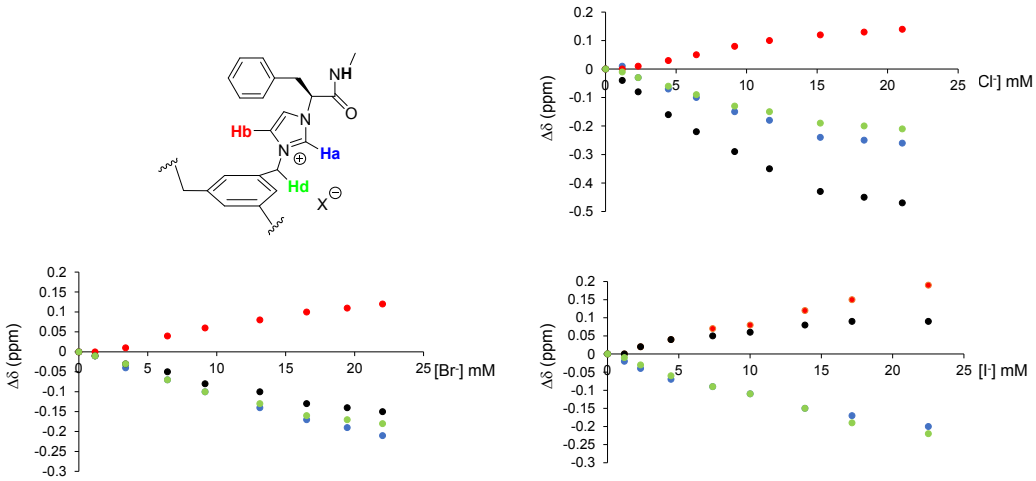

Figure S7. Plot of Δδ for compound [**1**]Br_3 *vs*. anion (Cl^-, Br^- and I^-) concentration

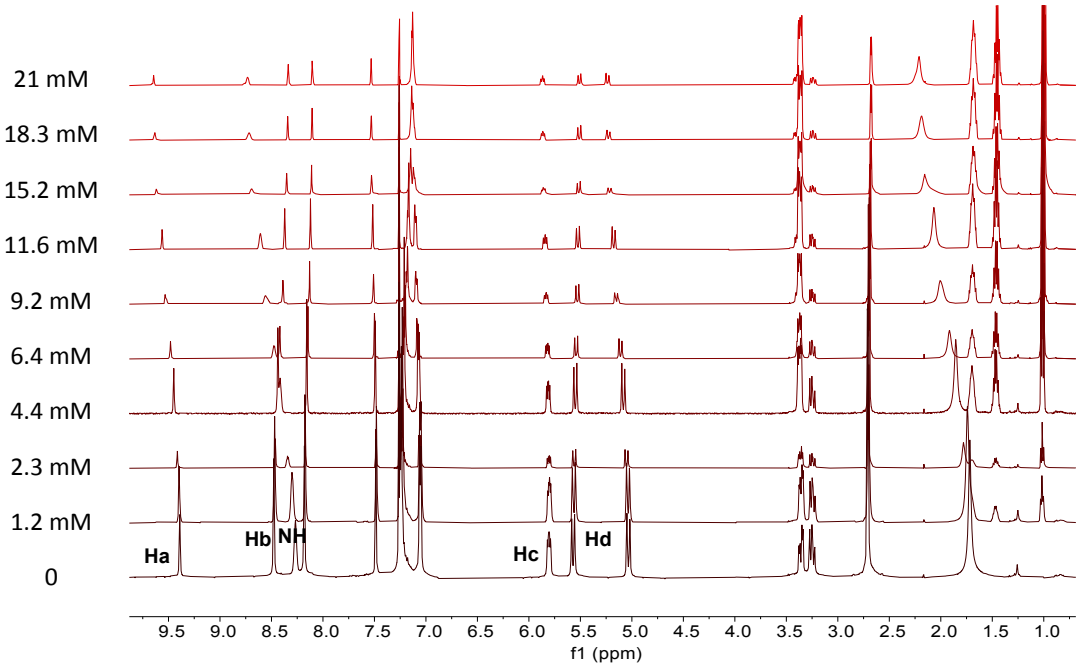

Figure S8. Partial ^{1}H NMR (500 MHz at 30^{o}C) of the compound [**1**]Br$_{3}$ (6 mM in $CDCl_3$) in the presence of different amounts of n-Bu_4NCl.

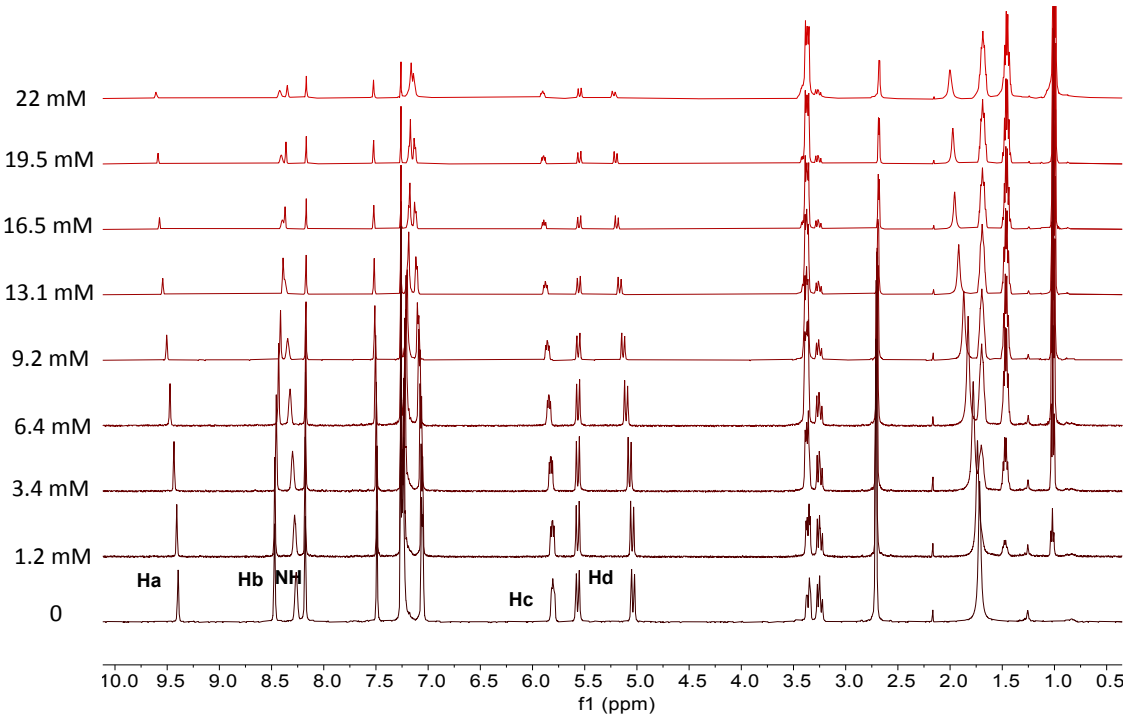

Figure S9. Partial ^{1}H NMR (500 MHz at 30^{o}C) of the compound [**1**]Br$_{3}$ (6 mM in $CDCl_3$) in the presence of different amounts of n-Bu_4NBr.

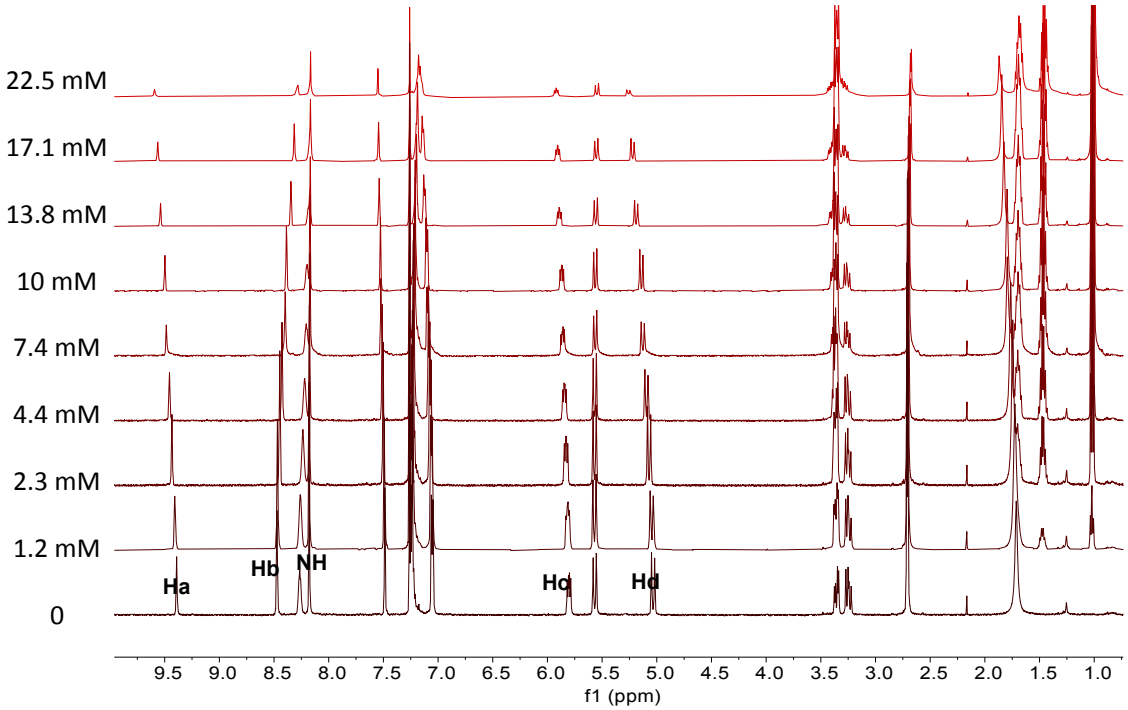

Figure S10. Partial ^{1}H NMR (500 MHz at 30^{o}C) of the compound [**1**]Br_3 (6 mM in $CDCl_3$) in the presence of different amounts of n-Bu_4NI.

6 Computational Details.

Calculations were performed using Gaussian16.[6] All geometries for model system were fully optimized using density functional theory (DFT) by means of the B3LYP functional[7] and DEF2TZVP basis set.[8] Analytical frequencies were calculated at the same optimization level in all cases, and the nature of the stationary points were determined in each case according to the proper number of imaginary frequencies. Initially, a Monte Carlo conformational search a search without constraints for every structure. The torsion angles were randomly varied, and the obtained structures were fully optimized using the MMFF force field.[9] Thus, 100 minima of energy within an energy gap of 10 kcal mol^{-1} were generated. These structures were analysed and ordered considering the relative energy, finally all repeated geometries were eliminated. In all cases, molecules with the lowest energy and an energy gap of 4.0 kcal mol^{-1} were selected and studied at the B3LYP/ DEF2TZVP level of theory.

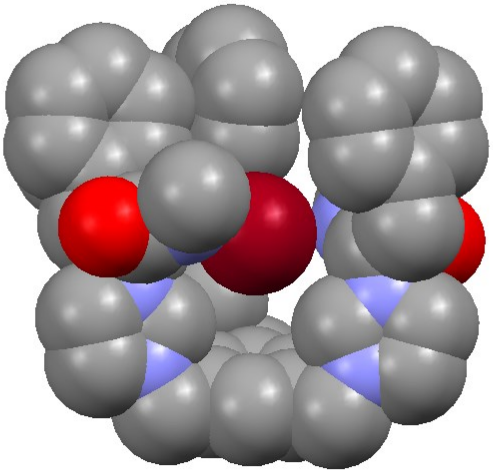

Figure S11. Space filling representation of the geometry minimized structure for the [**1** + Br]$^{2+}$ dication

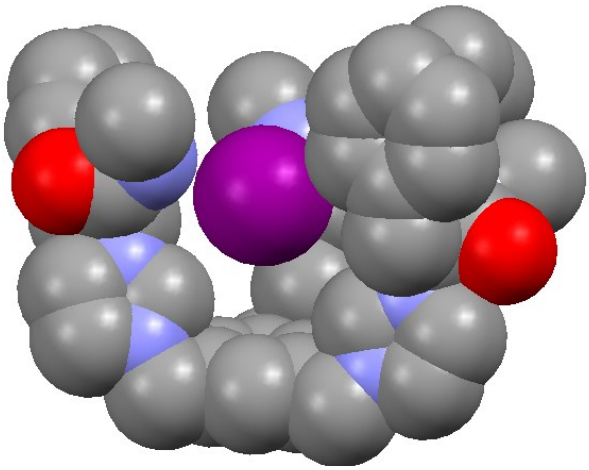

Figure S12. Space filling representation of the geometry minimized structure for the [**1** + I]$^{2+}$ dication

7 References

(1) Valls, B. Altava, M. I. Burguete, J. Escorihuela, V. Martí-Centelles, S. V. Luis, Org. Chem. Front. 2019, 6, 1214-1225

(2) Ruotolo, B. T.; Benesch, J. L. P.; Sandercock, A. M.; Hyung, S. J.; Robinson, C. V. *Nat. Protoc.* **2008**, *3*, 1139.

(3) Bush, M. F.; Campuzano, I. D. G.; Robinson, C. V. *Anal. Chem.* **2012**, *84*, 7124.

(4) Williams, J. P.; Scrivens, J. H. *Rapid Commun. Mass Spectrom.* **2008**, *22*, 187.

(5) (a) Coots, J.; Gandhi, V.; Onakoya, T.; Chen, X.; Andaluz, C. L. *J Aerosol Sci* **2020**, 105570; b) H. Kim, H. I. Kim, P. V. Johnson, L. W. Beegle, J. L. Beauchamp, W. A. Goddard, I. Kanik. *Anal. Chem.* 2008, 80, 1928-1936.

(6) Gaussian 16, Revision B.01, M. J. Frisch, G. W. Trucks, H. B. Schlegel, G. E. Scuseria, M. A. Robb, J. R. Cheeseman, G. Scalmani, V. Barone, G. A. Petersson, H. Nakatsuji, X. Li, M. Caricato, A. V. Marenich, J. Bloino, B. G. Janesko, R. Gomperts, B. Mennucci, H. P. Hratchian, J. V. Ortiz, A. F. Izmaylov, J. L. Sonnenberg, D. Williams-Young, F. Ding, F. Lipparini, F. Egidi, J. Goings, B. Peng, A. Petrone, T. Henderson, D. Ranasinghe, V. G. Zakrzewski, J. Gao, N. Rega, G. Zheng, W. Liang, M. Hada, M. Ehara, K. Toyota, R. Fukuda, J. Hasegawa, M. Ishida, T. Nakajima, Y. Honda, O. Kitao, H. Nakai, T. Vreven, K. Throssell, J. A. Montgomery, Jr., J. E. Peralta, F. Ogliaro, M. J. Bearpark, J. J. Heyd, E. N. Brothers, K. N. Kudin, V. N. Staroverov, T. A. Keith, R. Kobayashi, J. Normand, K. Raghavachari, A. P. Rendell, J. C. Burant, S. S. Iyengar, J. Tomasi, M. Cossi, J. M. Millam, M. Klene, C. Adamo, R. Cammi, J. W. Ochterski, R. L. Martin, K. Morokuma, O. Farkas, J. B. Foresman, and D. J. Fox, Gaussian, Inc., Wallingford CT, 2016.

(7) (a) C. Lee, W. Yang and R. G. Parr, Phys. Rev. B: Condens. Matter, 1988, 37, 785-789; (b) A. D. Becke, J. Chem. Phys., 1993, 98, 1372-1377; (c) A. D. Becke, J. Chem. Phys., 1993, 98, 5648–5652.

(8) F. Weigend, "Accurate Coulomb-fitting basis sets for H to Rn," Phys. Chem. Chem. Phys., 8 (2006) 1057-1065.

(9) (a) T. A. Halgren, J. Comput. Chem., 1996, 17, 490-519; (b) T. A. Halgren, J. Comput. Chem., 1996, 17, 520–552; (c) T. A. Halgren, J. Comput. Chem., 1996, 17, 553-586; (d) T. A. Halgren and R. B. Nachbar, J. Comput. Chem., 1996, 17, 587-615; (e) T. A. Halgren, J. Comput. Chem., 1996, 17, 616–641; (f) T. A. Halgren, J. Comput. Chem., 1999, 20, 720-729; (g) T. A. Halgren, J. Comput. Chem., 1999, 20, 730–748.